applied sciences

MDPI

Article

Drainage Troughs as a Protective Measure in Subway–Pedestrian Collisions: A Multibody Model Evaluation

Daniel Hall [1,*], Kevin Gildea [2] and Ciaran Simms [1]

[1] Department of Mechanical, Manufacturing and Biomedical Engineering and Trinity Centre for Biomedical Engineering, Trinity College Dublin, D02 PN40 Dublin, Ireland; csimms@tcd.ie
[2] Department of Technology & Society, Faculty of Engineering, Lund University, 221 00 Lund, Sweden; kevin.gildea@tft.lth.se
* Correspondence: hallda@tcd.ie

Featured Application: Evaluating the effect of train impact velocity, pedestrian position, and station environment on head injury and run-over risk. Application to future safety device design.

Abstract: Introduction: Subway–pedestrian collisions are a significant and growing problem, but they are poorly understood. This study presents the first subway–pedestrian collision model with the aim of evaluating the baseline safety performance of an R160 NYC train and track combination and the potential safety effects of drainage trough depth. Methods: A baseline simulation test sample of 384 unique impacts (8 velocities (2–16 m/s), 24 positions (standing jumping and lying), and 2 track types (flat and crossties)) was created in MADYMO. The full simulation test sample (N = 1920) included with various depth drainage troughs (0–1 m). Head injuries and wheel and third rail contacts were evaluated. Results: Limb–wheel contact occurred in 60% of scenarios. Primary and secondary contact HIC_{15} showed similar high severity, with an HIC_{15} < 2000 (88% risk of AIS 4+) in 29% of results for both train and ground contact. Impact velocity strongly influences primary contact HIC_{15} with limited effect on secondary contact. Impact velocities between 6 and 16 m/s showed little change in wheel contact. Increasing the trough depth up to 0.5 m showed a decrease in wheel contact probability with little increase in secondary contact. No further benefits were found above 0.5 m. Conclusions: A subway–pedestrian collision model is presented which predicts that wheel–pedestrian contact risk can be reduced with a 0.5 m drainage trough. The model suggests that slower impact velocities may reduce head injury risk for primary contact; however, this will have less effect on injuries caused by secondary and wheel contact.

Keywords: pedestrian safety; multibody modelling; head injury risk; subway train; rail safety; simulation

Citation: Hall, D.; Gildea, K.; Simms, C. Drainage Troughs as a Protective Measure in Subway–Pedestrian Collisions: A Multibody Model Evaluation. *Appl. Sci.* **2024**, *14*, 10738. https://doi.org/10.3390/app142210738

Academic Editor: Krzysztof Zboiński

Received: 25 September 2024
Revised: 5 November 2024
Accepted: 13 November 2024
Published: 20 November 2024

1. Introduction

The high number of pedestrian deaths worldwide is a well-documented problem, with the World Health Organization reporting 280,000 pedestrian fatalities in 2022 [1]. Extensive research has been conducted to improve pedestrian road vehicle safety, e.g., [2–6]. However, much less attention has been given to pedestrian incidents involving subway trains, despite deaths per 1,000,000 train miles increasing from 1.1 to 2.1 in the United States from 2013 to 2023 [7]. Existing subway crashworthiness research has focused on occupant protection (e.g., [8–13]) for subway vehicles and does not address subway–pedestrian collisions. There is thus a lack of published literature regarding this form of rail incident.

In automotive research, significant safety advances have been achieved by combining accident data analysis, physical testing, computational modelling, and accident reconstruction. For example, car-to-bicycle crashes have been evaluated using four different real world crash databases such as the German In-Depth Accident Study (GIDAS) [14]. The GIDAS database has often been used to inform multibody modelling initial conditions [15]. Data

from full-scale vehicle impact tests involving either a human dummy or a Post-Mortem Human Surrogate (PMHS), e.g., [16–18], can be used for model validation. Optimum impact parameters to reduce pedestrian risk have been evaluated using Multibody Modelling (MB), Finite Element (FE) modelling, or coupled FE and MB models, e.g., [19–21]. Weighted injury costs from multibody injury criteria have been used to assess the effects of vehicle shape and braking on pedestrian injury outcomes [22].

A major challenge in replicating this approach for subway safety is the cost of physical impact tests. Automotive pedestrian ground contact typically involves interaction with a flat surface [2,20,23]. Recent street-level tram–pedestrian collision studies utilize flat surfaces for secondary impact [24], or focus only on primary contact injuries [25]. In contrast, secondary contact for subway–pedestrian collisions involve a more complex geometry with different track types. These tracks introduce new dangers such as live electrically charged running rails (third rail), sharp corners, and drainage troughs, which may affect kinematics and run-over risk.

Drainage troughs (sometimes colloquially referred to as "suicide pits") are channels between the tracks allowing for extra space such that an individual may avoid contact with the train's undercarriage or wheels. Recent analysis of NYC incident reports shows a substantial number of cases with incapacitating injuries including amputation, likely resulting from wheel contact [26]. First used in the London Underground in 1932 [27], drainage troughs are present in many subway systems worldwide. Multiple analyses [28–30] of the effect of drainage show that troughs show lower fatality rates in stations featuring them. However, a recent paper showed a decline in references to these troughs since 2007 [31]. While empirical evidence suggests that drainage troughs may act as a viable countermeasure in reducing fatality rates, the results of such studies were unable to attribute the reduction in fatality rates to drainage troughs due to the presence of confounding factors [32].

There have been no proposed baseline models of subway–pedestrian interactions and there is no biomechanical analysis on the effect of drainage troughs on these events. While infrastructure such as Platform Screen Doors (PSDs) has been installed in modern subway systems, only 8.5% of NYC subway platforms were deemed feasible for this approach as of 2020, with this number increasing to a maximum of 27% by 2033 [33]. This warrants continued research into subway pedestrian safety. In particular, further research is needed to better quantify the effect of drainage troughs on pedestrian safety. Of particular interest is the required drainage trough depth to prevent wheel–pedestrian and third rail (high voltage) contact risk and the potential effect on secondary head impact injury.

The aim of this paper is therefore to use the multibody modelling software MADYMO (version 7.8) to create a New York City (NYC) subway–pedestrian model. The New York City Subway system is one of the largest in the world, with 5.5 million daily passengers and 185 subway train–pedestrian collisions in 2019 [26]. The purpose of the model is to provide biomechanical insights into:

- The effect of impact velocity on train–pedestrian run-over risk.
- The effect of drainage trough depth on third rail contact and run-over probability as well as the minimum trough depth needed to avoid wheel or undercarriage contact.
- The effect of impact velocity on both primary and secondary contact head injury risk.

2. Materials and Methods

Multibody modelling and injury weighting methods were used to create the baseline model and assess the effects of speed, third rail, and drainage troughs on injury outcome. Accordingly, the methodology addresses the following

- Multibody Train and Station Environments (2 track types)
- Adapted Multibody Pedestrian Model (AM50)
- Pedestrian Posture and Train Speed
- Simulation Test Sample (STS) with Injury Criteria, Contact Scores, and Weighted Scoring
- Sensitivity Study

2.1. Multibody Train Model and Impact Velocity

The R160 train has the largest fleet within the NYC subway system (>1600 trains) and is associated with the highest number of fatal subway–pedestrian interactions in the NYC Subway in 2019 [26]. The multibody R160 train front was created in MADYMO using thirteen cylinders and fourteen ellipsoids based on dimensions supplied by the Federal Transit Administration (Figure 1). The train front was split into eight separate groups for contacts (front panels, door, window, anti-climber, coupler, wheels, truck, and undercarriage). As the train front is significantly stiffer than the human model, the contact characteristics used were those of the MADYMO pedestrian model, i.e., the train was treated as completely rigid. The track geometry simulated for this study is shown in Figures 2 and 3.

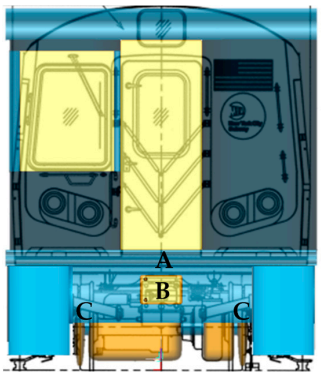

Figure 1. MADYMO multibody model of an R160 subway train. A = anticlimber, B = coupler, and C = wheels.

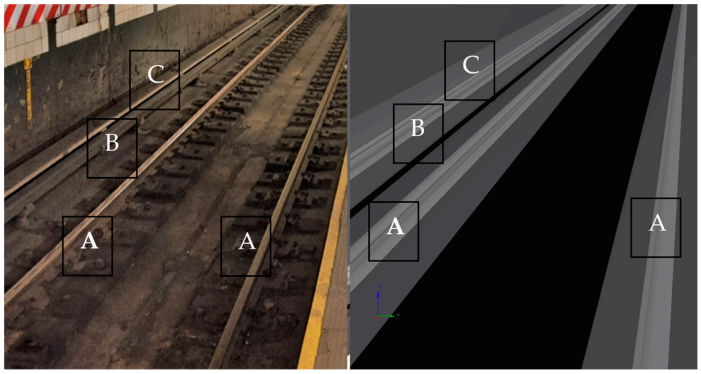

Figure 2. NYC flat track bed with no crossties (image taken by the author) and multibody model. A—running rail, B—third rail (live), and C—third rail guard.

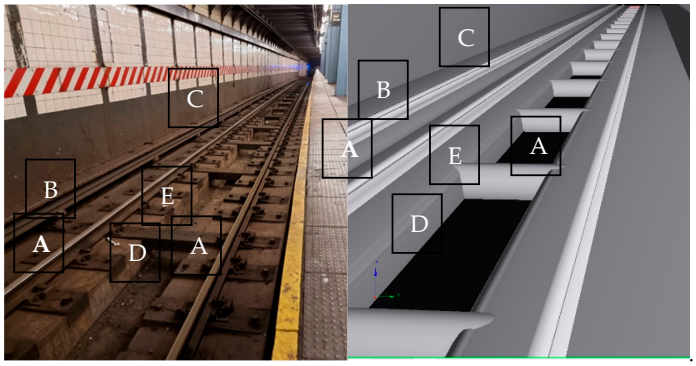

Figure 3. NYC track bed with drainage trough and crossties (image taken by the author) and multibody model. A—running rail, B—third rail (Live), C—third rail guard, D—drainage trough (suicide pit), and E—crosstie.

The most common estimated subway–pedestrian impact velocity is 40–47 km/h, but low impact velocity may also be fatal due to the stiffness of the train front and the possibility of wheel or third rail contact [26]. The impact velocities used in this study therefore range from 2 to 16 m/s in 2 m/s increments [26]. Based on the available NYC event recorder data supplied as part of a 2019 incident report analysis study [26], the R160 train's emergency braking was modelled as a linear deceleration of 1.43 m/s^2.

2.2. Adapted MADYMO Human Pedestrian Model

The MADYMO pedestrian models are often used in kinematic studies involving automotive pedestrian impacts [2,34,35]. Epidemiological studies found the average age and sex distribution of 941 fatal NYC subway human collisions from 1990–2007 [28,29] and 2019 [26,36,37] as 83% male with a mean age range of 35–45 years old. Based on these findings, the MADYMO Adult Male 50th Percentile (AM50) ellipsoid model was chosen. This model has been used extensively to assess the influence of vehicle impact velocity and pedestrian posture during vehicle contact e.g., [34,38].

The MADYMO AM50 model consists of 52 rigid bodies connected by a kinematic joint. Additionally, frangible joints are present in the legs to account for fracture. By default, these joints remain locked until a fracture threshold is met, following which the connected segments are free to rotate relative to each other. The AM50 model applies minor damping forces to prevent numerical instabilities caused by gimbal lock, a phenomenon where two rotational axes align and eliminate a degree of freedom, causing numerical problems. However, preliminary analysis showed that due to the high impact force and complex positioning used in this study, this damping force was insufficient to prevent gimbal lock. Given the high likelihood of amputation caused by contact with a moving subway train wheel, limb fracture was not the focus of this study. Thus, these joints remained locked to allow simulations to run to completion and focus on head injuries. A sensitivity study was conducted to assess the effect of this on the overall findings.

To address the limited head contact data available for model validation, the default MADYMO AM50's head contact characteristics were altered to reflect those calculated based on the ground contact for 6 published PMHS tests [2].

2.3. Pedestrian Position and Pose

Pedestrian impacts are highly sensitive to initial conditions, with minor changes in pedestrian pre-impact pose sometimes having a significant effect (e.g., change of head contact location from a soft to a stiff region) [39]. To improve the validity of our simulations, we sourced real-world videos and employed pose estimation techniques to define plausible pedestrian pre-impact poses. Firstly, 2D poses were manually annotated, defining the pixel coordinates for each key point on the pedestrian. GAST-Net was then applied to lift the 2D poses to 3D [40]. An inverse kinematics optimisation technique (KinePose) developed to infer joint orientations in a user-customisable biomechanical model for 3D pose estimates [41] has been previously applied to cyclist falls [42]. The approach was adapted for use in the study presented herein with the MADYMO ellipsoid models using reorientable joints [41]. The resulting poses are shown in Figure 4.

2.4. Simulation Test Sample (STS)

2.4.1. Full STS

A simulation test sample (STS) was developed to represent the range of possible impact configurations in subway–pedestrian incidents, using NYC incident report data [26] as the primary source. This resulted in 1920 unique Impact Scenarios (IS) across 24 positions, 8 velocities, 5 trough depths, and 2 track types. Furthermore, a weighting system was applied to also address the likelihood of each scenario [43]. This weighted STS was then used to assess the likelihood of wheel run-over across a range of impact positions, impact velocities, and track geometries. The full STS conditions are presented in Table 1.

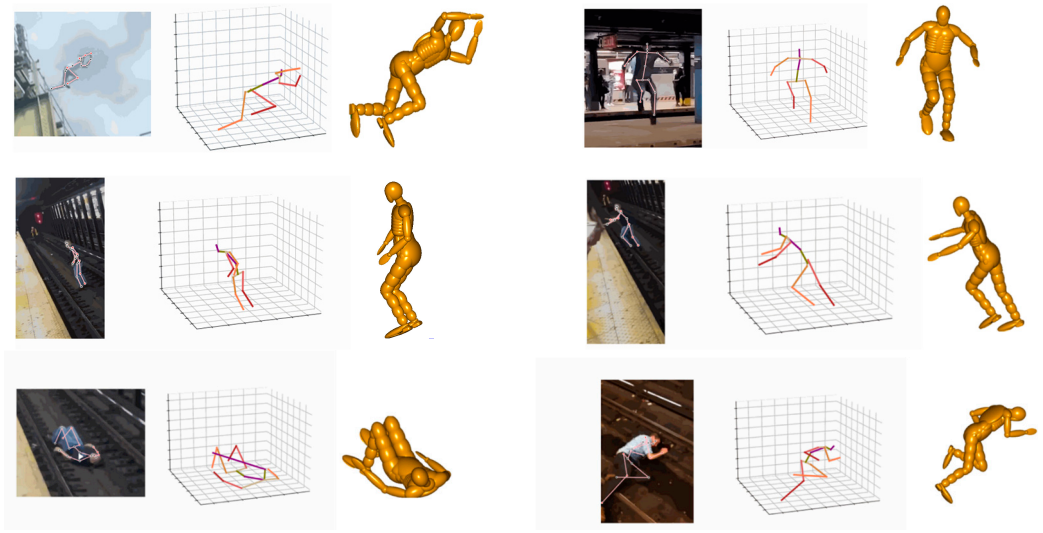

Figure 4. Representative stills from YouTube videos, illustrating 2D keypoints, 3D keypoints, and the subsequent MADYMO pedestrian modelling configuration via KinePose [41].

Table 1. Full simulation test sample conditions.

Impact Position	Postures	Impact Location	Track Type	Trough Depths (m)	Impact Velocities (m/s)	Total Simulations
Lying	Lying 1 Lying 2	Left Right Middle	Flat bed Crossties	5 [0 0.25 0.5 0.75 1]	8 [2 4 6 8 10 12 14 16]	2 × 3 × 2 × 5 × 8 = 480
Mid Jump	Jump 1 Jump 2	Left upper and lower Right upper and lower Middle upper and lower	Flat bed Crossties	5 [0 0.25 0.5 0.75 1]	8 [2 4 6 8 10 12 14 16]	2 × 6 × 2 × 5 × 8 = 960
Standing	Standing 1 Standing 2	Left Right Middle	Flat bed Crossties	5 [0 0.25 0.5 0.75 1]	8 [2 4 6 8 10 12 14 16]	2 × 3 × 2 × 5 × 8 = 480

2.4.2. Baseline Simulation Test Sample (BSTS)

A subset of this STS was used to develop the baseline (as-is) risk for comparison. This baseline simulation test sample (BSTS) consists of 24 impact positions, 8 velocities, and 2 track types but with only one trough depth for each track type (0 m for flat track bed (Figure 2) and 0.25 m for the track bed with crossties (Figure 3). This results in 384 impact scenarios representing the existing NYC subway environment. This BSTS allows for comparisons to be drawn between the existing environment and one with a different drainage trough depth and, in the future, potentially also the assessment of other proposed countermeasures.

2.5. Injury Criteria and Contact Scores (CS)

2.5.1. Head Injury Criteria (HIC)

The Head Injury Criterion (HIC_{15}) was used to quantify the head injury risk for each simulation [44]. HIC scores are frequently used in automotive safety research, e.g., [45,46]. The primary impact time window for distinguishing primary head contact from either secondary or run-over head contact was set at 0–0.4 s for lying, 0–0.5 s for jumping, and 0–0.28 s for standing impacts. An additional contact phase between the pedestrian and the train is present in IS, which involves run-over.

Based on the calculated HIC scores, the probability of Abbreviated Injury Scale (AIS) head injury risk was determined using correlation [47]. A nominal HIC_{15} threshold was set

at 2000, corresponding to an 88% probability of an AIS4+ injury, and this was chosen as a reasonable upper limit of survivability.

2.5.2. Contact Score (CS)

To investigate the effect of track geometry on electrocution by the third rail, a contact probability system was used. The contact score (CS) was defined as the number of simulations predicting at least one wheel/third rail contact, divided by the total number of simulations for that configuration. Wheel and third rail contacts were defined as a binary measure (1 for one or more contacts and 0 for no contacts).

2.6. Weighted Injury Score (WIS)

Not all impact scenarios occur at the same frequency [26]. NYC subway Public Transportation Safety Board (PTSB) case reports were used to calculate the proportional frequency of each simulated impact scenario [26]. There were 25 cases with both a recorded impact velocity between 2–16 m/s and a recorded impact position of either standing, jumping or lying. Over 40% of these incidents occurred at 12–14 m/s, while only 4% occurred at 14–16 m/s, indicating the need for a Weighted Injury System (WIS) and Weighted Contact Score (*WCS*).

The Impact Scenario Proportion *(ISP)* was defined as the product of the Impact Velocity Proportion *(IVP)* and Impact Position Proportion *(IPP)*, where the sum of each proportion is equal to 1 (Equations (1) and (2)). The Weighted Contact Score was defined as the sum of the products for the base *CS* with the associated ISP divided by the sum of the ISPs (Equation (3)).

$$ISP = IVP * IP \tag{1}$$

$$\sum_{i=1}^{N} ISP_i = \sum_{i=1}^{N} IVP_i = \sum_{i=1}^{N} IPP_i = 1 \tag{2}$$

$$WCS = \frac{\sum_{i=1}^{N} CS_i * ISP_i}{\sum_{i=1}^{N} ISP_i} \tag{3}$$

2.7. Sensitivity Study

A sensitivity study was conducted to assess the influence of contact hysteresis and fracture joint damping on the relationship between trough depth, run-over risk, and head injury risk. This assessment involved using a smaller subset of nine jumping impact scenarios.

3. Results

3.1. Sensitivity Study

The sensitivity study showed that the *CS*s vary by up to 30% with hysteresis; however, the general relationship between the *CS* and trough depth remains the same. In particular, with an increase in trough depth, the *CS*s drop regardless of the hysteresis value used (*CS* reduction ranges between 73 and 82%). These results indicate that the model predictions regarding the effect of drainage trough depth on run-over risk are not greatly influenced by energy absorption.

Direct comparison of how the *CS* or HIC scores are affected by fracture joint changes is not possible as the data are unavailable for simulations which failed due to gimbal lock. Locking the fracture joints allows all simulations to run to completion. As leg injuries are not considered, this approach was followed to allow the study to proceed. The following results are therefore based on the AM50 model with locked leg fracture joints.

3.2. Baseline Run-Over Risk

Figure 5 shows the *CS* and *WCS* for the baseline simulation test sample (BSTS). The modelling results suggest that a typical collision between an R160 subway train and a 50th percentile male pedestrian in the existing NYC track environment has a contact likelihood

of 59% for limb-to-wheel contact, 27% for body-to-wheel contact, 11% for head-to-wheel contact, and 23% for third rail contact.

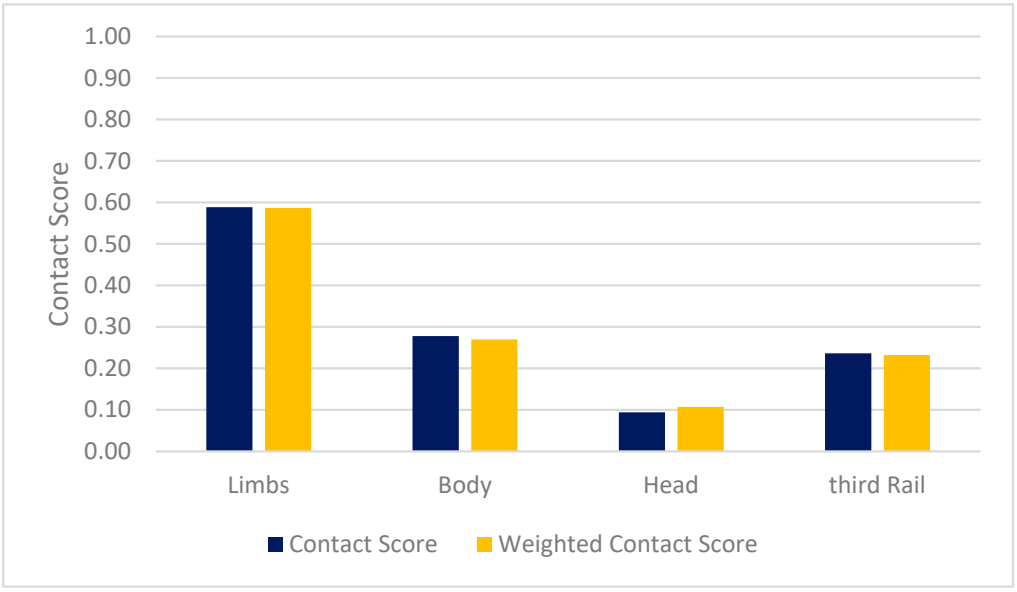

Figure 5. Overall combined contact scores and weighted contact scores for the baseline simulation test sample.

Figure 6 shows the BSTS contact and weighted contact score separated by impact conditions. Lying has the highest weighted contact score (*WCS*) across all regions while jumping IS show a relatively lower *WCS* for the limbs compared to lying or standing. The third rail contact scores are 0.2–0.3 for all impact positions.

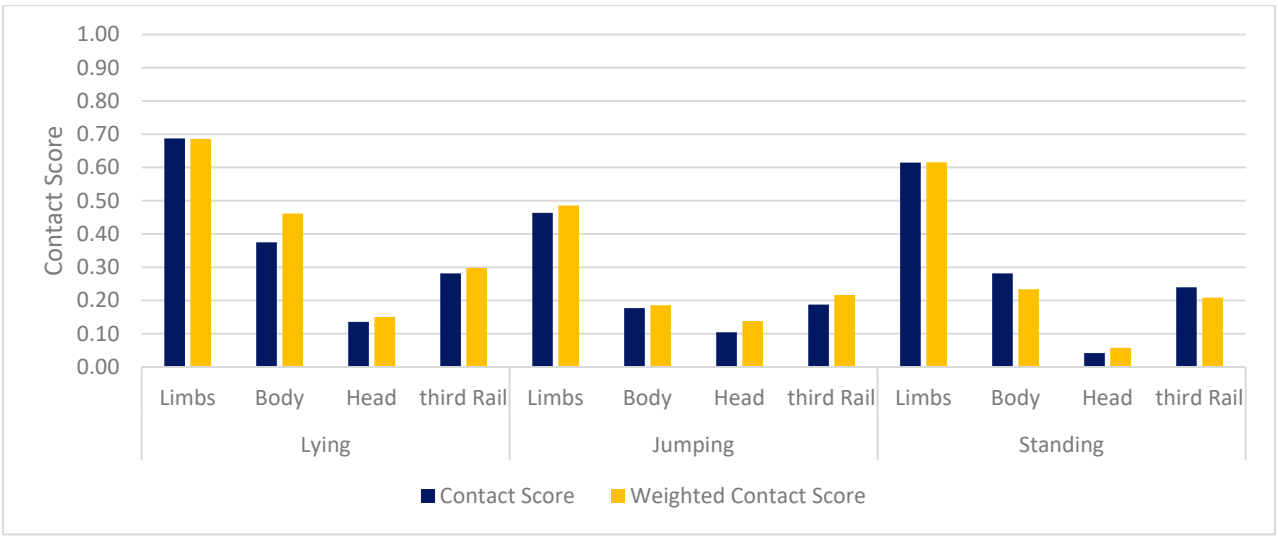

Figure 6. Contact scores and weighted contact scores for the baseline model for each impact position.

Figure 7 presents the relationship between the *CS* and impact velocity, where above a train speed of 4 m/s, the impact velocity does not greatly affect the contact scores. The weighted contact scores do not substantially differ from the unweighted contact scores, implying that the *CSs* are independent of impact position and velocity.

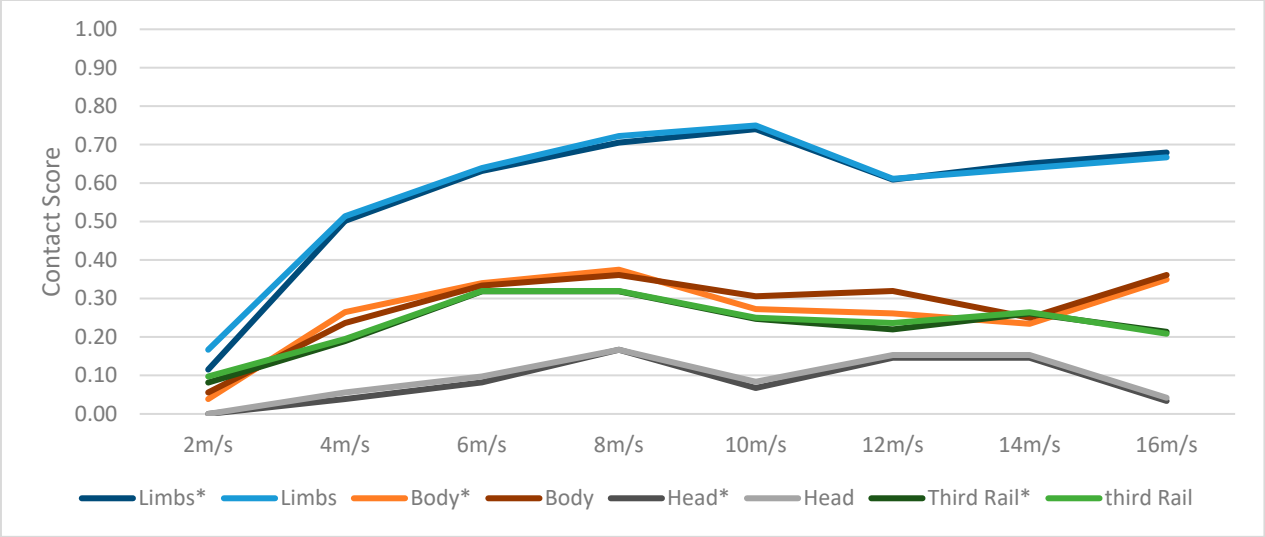

Figure 7. Contact scores and weighted contact scores shown as a function of impact velocity (weighted *).

3.3. Baseline Head Injury Risk

Figure 8 shows the range of primary and secondary HIC_{15} scores for the BSTS. The shaded region shown in each box and whisker plot represents the 95% confidence interval of the median value. The jumping *ISs* result in the highest range of HIC_{15} scores, while the standing *ISs* show a smaller range but higher HIC_{15} values. Secondary contacts show similar HIC_{15} scores in both jumping and standing and a lower dependency on impact velocity. HIC_{15} scores above the 2000 threshold correspond to a greater than 88% probability of AIS4+ head injury.

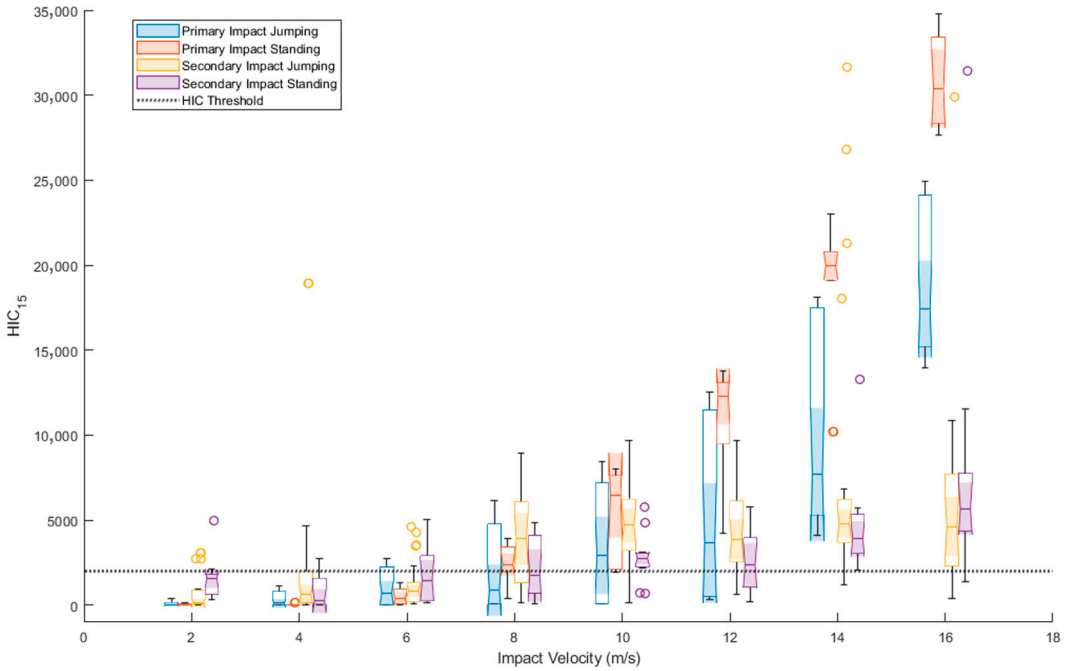

Figure 8. Baseline simulation test sample (BSTS) primary and secondary HIC_{15} scores for jumping and standing impacts. The 2000 HIC_{15} threshold is also shown.

Figure 9 shows the proportion of jumping and standing HIC_{15} scores that fall below the threshold HIC_{15} score of 2000. The models suggest that only 29% of incidents will result in an AIS4+ head injury probability of less than 88%. Primary impact shows a similar

proportion of cases below this threshold (47% compared to 44% for secondary contact HIC_{15} scores).

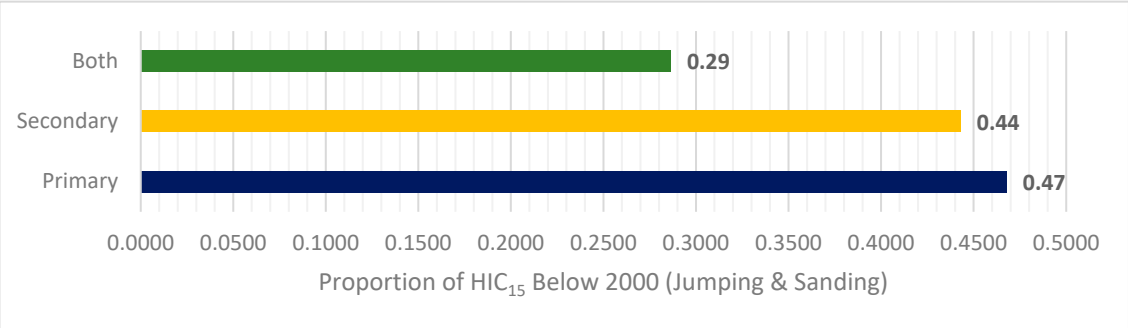

Figure 9. Baseline simulation test sample proportion of jumping and standing $HIC_{15} < 2000$.

3.4. STS Run-Over Risk

Figure 10 shows the relationship between drainage trough depth and wheel/third rail contact for the full simulation test sample. There is a general reduction in *CSs* with increasing drainage trough depth. This relationship is strongest for jumping, with less effect for standing or lying. Jumping scenarios also show the lowest *CS* for limbs, body, and third rail contact, with similar head *CSs* to standing. There is no clear relationship between drainage trough depth and wheel/third rail contact probability for lying. Overall, the model shows a general decline in wheel and third rail contact as trough depth increases for the limbs and, in some cases, for the head and body. This relationship is most prominent between 0–0.5 m of trough depth, with little to no additional benefit beyond 0.5 m.

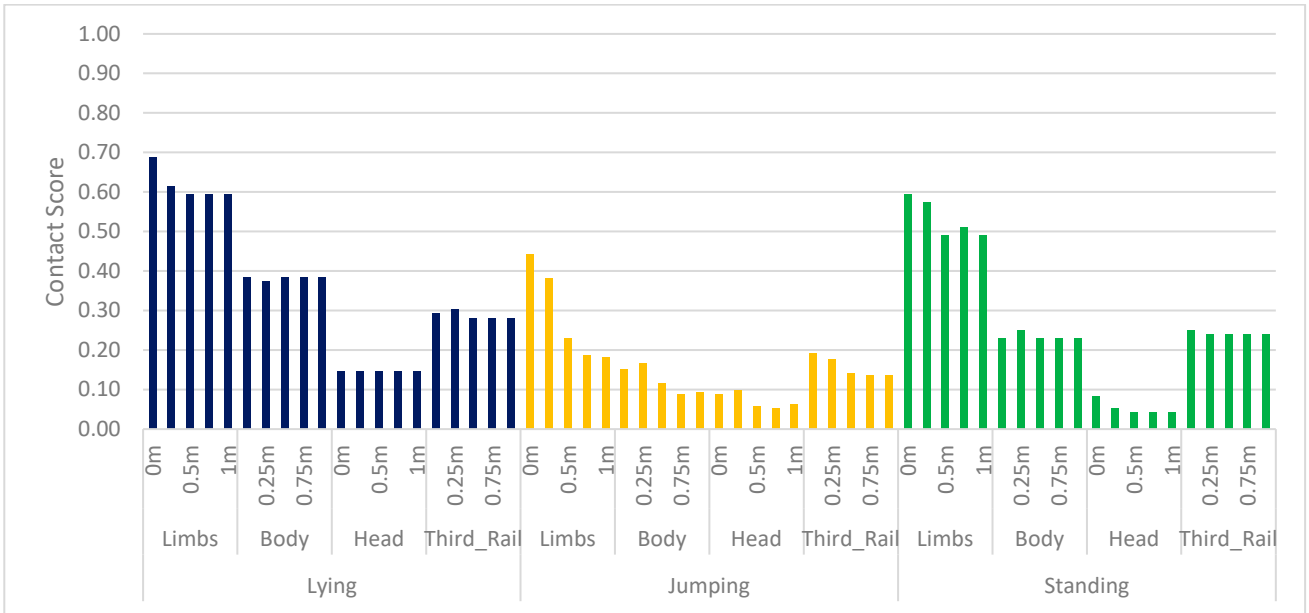

Figure 10. Full simulation test sample contact scores separated by impact position and drainage trough depth.

3.5. STS Head Injury Risk

Figure 11 shows the effect of drainage trough depth on secondary contact HIC_{15} score for jumping and standing scenarios. There are only small changes in the median HIC_{15} score with each increment in trough depth, but a significant difference with 95% confidence for jumping can be found when comparing HIC_{15} at 0 m and 1 m trough depth. The significance level is based on a normal distribution assumption.

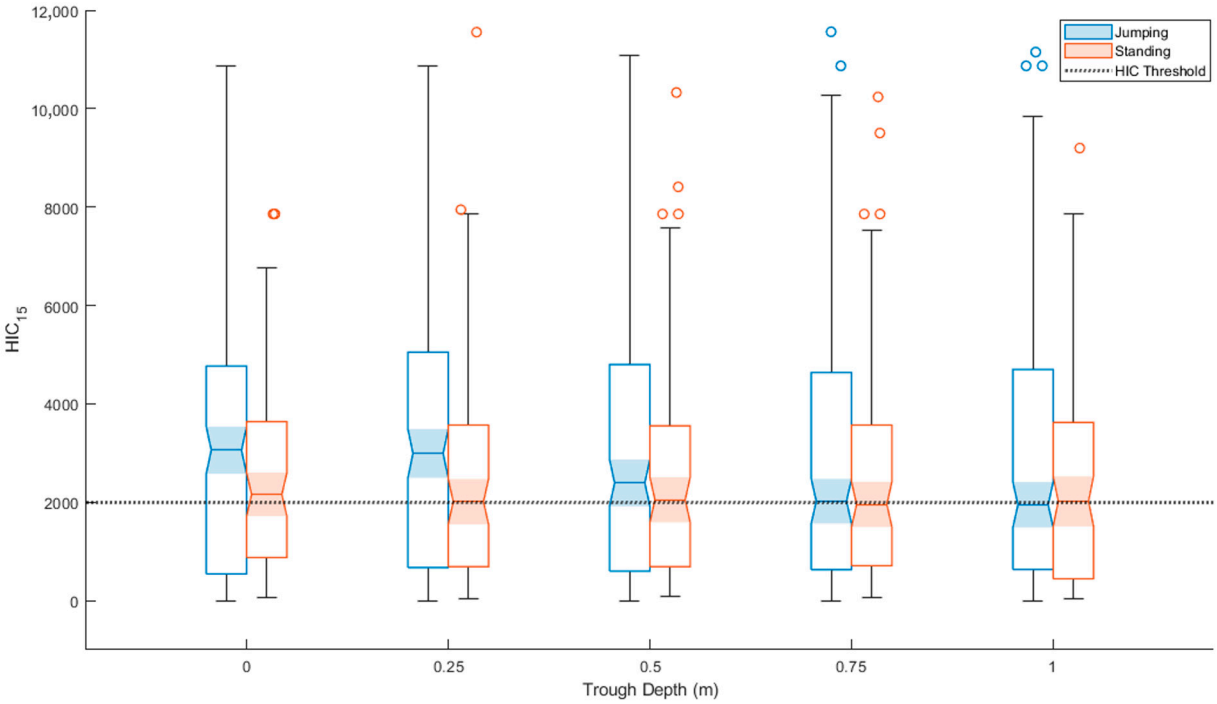

Figure 11. Relationship between drainage trough depth and secondary contact HIC_{15} score for jumping and standing impact scenarios.

4. Discussion

Subway–pedestrian collisions are becoming more frequent [7], but there is a lack of biomechanical analyses and proposed interventions. To the best of our knowledge, this is the first model of subway–pedestrian collision interactions. As there is no validation data against which to assess this model, predicted trends offer more significance than absolute values, similar to the approach taken in [48].

The sensitivity study shows that the trends in modelling results are not greatly sensitive to the uncertainty in contact hysteresis. Furthermore, locked leg fracture joints are required for modelling to proceed.

4.1. Main Findings

The risk of direct contact with the wheels is highest for the limbs and lowest for the head. Lying on the tracks is not surprisingly generally worse than jumping or standing (Figure 6), although this does not account for any voluntary movement such as intentional positioning in the centre of the track. The models therefore more closely resemble a pedestrian falling onto the tracks and not moving. Third rail contact occurs about 20% of the time; however, this is likely an overestimation due to high penetration into the third rail guard, which is a modelling limitation. There is a weak impact velocity dependency on contact scores for impact velocities above 4 ms^{-1} (Figure 7). There is a strong impact velocity dependency on primary contact HIC_{15} scores but not on secondary contact HIC_{15} (Figure 8), which is similar to findings from vehicle–pedestrian collisions [20]. Regarding head injury risk, about 30% of the Baseline Simulation Test Sample (BSTS) cases are potentially survivable, with a $HIC_{15} < 2000$ for both primary and secondary impacts (Figure 9). The contact scores decrease with drainage trough depth up to 0.5 m, with the largest benefit observed in jumping impact scenarios (Figure 10). Increasing the trough depth beyond 0.5 m shows little benefit. Trough depth shows a significant difference in secondary contact HIC_{15} between 0 and 0.5 m trough depth (Figure 11), and this is likely caused by a deeper trough reducing the likelihood of a pedestrian hitting the ground headfirst. This does not account for any potential change in other body region injuries.

4.2. Baseline Run-Over Risk

The current risk of a subway–pedestrian interaction resulting in a limb amputation is almost 60% for the full baseline impact scenarios (Figure 5). The pre-impact position is an influencing factor in calculating this risk. The limb contact risk varies between 69% and 46% for lying and jumping impact scenarios, respectively (Figure 6). The high contact scores for lying impact scenarios are expected as the left and right lying positions are in the direct path of the train wheels for primary contact. The standing and jumping impact scenarios result in a primary impact location higher up on the train front, requiring an additional train contact phase for run-over to occur. Potential actions taken by the pedestrian to avoid contact (such as lying between the rails) have not been modelled, as the models are passive.

Figure 7 shows that impact velocity has a marginal influence on contact scores. Impact velocities between 6 and 16 m/s show little to no change in contact scores. However, the contact score is significantly lower between 2 and 4 m/s. This may be caused by the complete absence of a run-over due to the emergency braking of 1.43 m/s^2. This suggests that train–pedestrian impacts pose similar run-over risks independent of the impact velocity at speeds above 4 m/s. A recent study found that the most common impact velocity on the NYC subway was 12 m/s [26]. This suggests that this impact velocity must be decreased to below 4 m/s before any substantial benefit will be found in reducing pedestrian–wheel contact injuries. Given the passive nature of the pedestrian models, the lower velocity (<4 m/s) contact scores are likely an overestimation as no active avoidance manoeuvres are made by the pedestrian model. During a real pedestrian collision at 2 m/s, sufficient time might be available to physically manoeuvre into a more advantageous position. At higher impact velocities, the ability to move out of the path of the wheels is less likely.

4.3. Effect of Drainage Trough Depth on Run-Over Risk

Figure 10 shows that contact scores for jumping impact scenarios are heavily influenced by drainage trough depth. The limb contact score falls from 44% to 18% as the trough depth increases from 0 to 1 m. Contact scores from standing and lying show less dependency on trough depth. The secondary contact phase for a jumping pedestrian occurs later than for standing and lying. This yields two benefits: there is additional time for the train to decelerate before run-over can occur and there is more time for the pedestrian to fall into the trough before roll-over.

The greatest change in contact scores can be seen between as trough depth increases from 0–0.5 m, while additional trough depths yield little further benefit. This is likely due to the secondary contact position of the pedestrian. Cases which yielded no benefit from a 0.5 m trough due to their secondary contact positioning are unlikely to benefit from a 1 m trough. Conversely, pedestrians who avoided the train due to a 0.5 m trough will not further benefit from a 1 m trough. Third rail contact does not significantly depend on trough depth, with a 2% reduction between 0 and 0.5 m, and the contact score for third rail contacts remains between 20 and 25% for the full simulation test sample. Due to the nature of rigid multibody modelling, this is likely an overestimation as the pedestrian's limbs or other body regions cannot be severed. This can cause the pedestrian in the model to be dragged along the rails, increasing the likelihood of third rail contact. Overall, a drainage trough with a depth of 0.5 m may reduce the risk of wheel–pedestrian contact but will offer no benefit for third rail contact prevention. Future studies optimising the geometry of the trough through both width, depth, and curvature may offer further insights into the safety benefit. This research could be used to inform future track design policy.

4.4. Baseline Head Injury Risk

Figure 8 shows a strong dependency of primary impact HIC_{15} score on train impact velocity, while secondary impact HIC_{15} scores show little velocity dependency between 6 and 16 m/s. Impact velocities between 12 and 16 m/s show a significant difference with 95% confidence in the median primary HIC_{15} scores for jumping (lower primary HIC_{15} scores) compared to standing (higher primary HIC_{15} scores) impacts. There are more

outliers detected for secondary contacts as the variability in impact conditions is much greater, as previously observed for secondary contact for vehicle–pedestrian collisions [20].

Figure 9 shows that 29% of the jumping and standing impacts result in a HIC_{15} score of less than 2000 for both primary and secondary impacts. This implies that countermeasure design must incorporate both primary and secondary impact mitigation to be effective.

Figure 11 shows that the secondary contact HIC_{15} surprisingly decreases with trough depth. Upon further investigation, it was found that the addition of the trough changes the kinematics of the ground contact reducing the likelihood of headfirst collisions, thus reducing pedestrian head–ground contact velocity. This does not account for any change in injury probability associated with other body regions, such as the chest or spine. Regarding HIC_{15} scores alone, these findings show no negative consequence of increasing trough depth.

4.5. Limitations

There are several limitations to this work. The lack of experimental data needed for model validation means that the results are focused on trends rather than individual simulations. However, the sensitivity study to assess the dependency of these trends on unknown factors showed no significant reliance. Future model validation research utilizing full-scale staged tests would be most beneficial; however, the financial cost of such tests would be high. Retrospective injury analysis of similar impact cases to those used in the STS would advance model validation; however, NYC medical examiner records and injury data were not available at the time of this study. While multibody modelling allowed for a large simulation test sample to be evaluated, it prevented the simulation of deformations and amputations, meaning that decapitations and bisections could not be modelled. This may cause an overestimation of third rail contact likelihood as the body can be dragged alongside the train instead of becoming separated from the body region in contact with the wheels. Furthermore, the subway environment includes more sharp or edge contacts compared to automotive collisions. For primary contact, potential sharp interactions include the anticlimber, coupler, and train wheels. For secondary contact, sharp interactions could include the rails, crossties, and trough edges. The contact characteristics used in this study are based on force–penetration relationships and as such, any change in head acceleration due to the object's geometric sharpness is not considered in head injury risk calculations. The initial conditions, track environment, and train front geometry used in this study are based on the NYC subway system. At the time of the study, the NYC subway is one of the largest subways in the world and offers the most up-to-date pedestrian incident information [26]. However, to represent the growing global issue of subway–pedestrian collisions, further studies using different pedestrian characteristics such as sex, height, and weight as well as track and train types are needed, and this will be the focus of future work.

Notwithstanding these limitations, this paper offers the first model of subway–train interactions and assesses the effect of drainage troughs as a potential means of improving pedestrian safety.

5. Conclusions

A model of subway–pedestrian collisions is presented, taking into account variability in impact configurations. The model predicts a substantial risk of wheel contact during run-over and shows this is not strongly speed dependent, except at very low speeds. On the other hand, increasing the drainage trough depth reduces the likelihood of contact with both the wheel and the third rail. Furthermore, the model shows that increasing the drainage trough depth does not significantly influence the injury risk in secondary contact with the ground. Similar to vehicle–pedestrian collisions, primary contact with the subway is much more sensitive to subway speed than secondary contact with the ground. Finally, the high injury severity predicted by the model for both primary and secondary contact indicates that pedestrian protection interventions must address both

of these impact phases. The results of this model offer a baseline injury risk against which future countermeasure studies may be compared. For potential subway–pedestrian safety advancements, roll-over likelihood would be reduced with the implementation of a drainage trough with a minimum depth of 0.5 m. This may inform future subway track design policies incorporating pedestrian safety into drainage trough systems. Reducing the approach velocity of incoming subway trains into the station would decrease primary contact head injury risk, but a substantial velocity reduction (station entry velocity < 4 m/s) would be required to reduce run-over likelihood. Countermeasures to address secondary contact head injury risk are required. Future studies of track guards utilizing the available drainage trough space while providing softer ground contact surfaces may be a promising area of research.

Author Contributions: Conceptualization, D.H. and C.S.; methodology, D.H. and C.S.; software, D.H. and K.G.; validation, D.H., C.S. and K.G.; formal analysis, D.H. and C.S.; investigation, D.H. and C.S.; resources, D.H.; data curation, D.H.; writing—original draft preparation, D.H.; writing—review and editing, D.H., K.G. and C.S.; visualization, D.H.; supervision, C.S.; project administration, C.S.; funding acquisition, C.S. All authors have read and agreed to the published version of the manuscript.

Funding: This research is funded by the FTA under FTA-2020-004-TRI-SRD: Research effort entitled "FY20 SRD-Designed for Impact—An Innovative Approach to Train Safety and Collision Fatality Reduction".

Institutional Review Board Statement: Not applicable.

Informed Consent Statement: Not applicable.

Data Availability Statement: The original contributions presented in the study are included in the article, further inquiries can be directed to the corresponding author.

Acknowledgments: Tom Lamb—providing support and the R160 dimensions used to create the train model. Logan Zentz, Bronislaw Gepner, Katarzyna Rawska, and Greg Shaw at the University of Virginia—offering useful modelling advice and guidance.

Conflicts of Interest: The authors declare no conflicts of interest.

References

1. WHO. Death on the Roads. Available online: https://extranet.who.int/roadsafety/death-on-the-roads/#ticker/all_road_users (accessed on 12 November 2024).
2. Shang, S.; Masson, C.; Llari, M.; Py, M.; Ferrand, Q.; Arnoux, P.-J.; Simms, C. The predictive capacity of the MADYMO ellipsoid pedestrian model for pedestrian ground contact kinematics and injury evaluation. *Accid. Anal. Prev.* **2021**, *149*, 105803. [CrossRef] [PubMed]
3. Martin, A. *Factors Influencing Pedestrian Safety: A Literature Review*; TRL: Wokingham, UK, 2006.
4. Kerrigan, J.R.; Crandall, J.R.; Deng, B. Pedestrian kinematic response to mid-sized vehicle impact. *Int. J. Veh. Saf.* **2007**, *2*, 221–240. [CrossRef]
5. Tiwari, G. Progress in pedestrian safety research. *Int. J. Inj. Control Saf. Promot.* **2020**, *27*, 35–43. [CrossRef] [PubMed]
6. Combs, T.S.; Sandt, L.S.; Clamann, M.P.; McDonald, N.C. Automated vehicles and pedestrian safety: Exploring the promise and limits of pedestrian detection. *Am. J. Prev. Med.* **2019**, *56*, 1–7. [CrossRef] [PubMed]
7. Federal Railroad Administration. Accident Trends: Charts & Graphs, Trespasser Casualty Rate. Available online: https://safetydata.fra.dot.gov/officeofsafety/publicsite/graphs.aspx (accessed on 12 November 2024).
8. Han, H.-S.; Koo, J.-S. Simulation of train crashes in three dimensions. *Veh. Syst. Dyn.* **2003**, *40*, 435–450. [CrossRef]
9. Xue, X.; Schmid, F.; Smith, R. Analysis of the structural characteristics of an intermediate rail vehicle and their effect on vehicle crash performance. *Proc. Inst. Mech. Eng. Part F J. Rail Rapid Transit* **2007**, *221*, 339–352. [CrossRef]
10. Li, R.; Xu, P.; Peng, Y.; Xie, Y.-q. Scaled tests and numerical simulations of rail vehicle collisions for various train sets. *Proc. Inst. Mech. Eng. Part F J. Rail Rapid Transit* **2016**, *230*, 1590–1600. [CrossRef]
11. Peng, Y.; Hou, L.; Yang, M.; Tian, H. Investigation of the train driver injuries and the optimization design of driver workspace during a collision. *Proc. Inst. Mech. Eng. Part F J. Rail Rapid Transit* **2017**, *231*, 902–915. [CrossRef]
12. Xu, P.; Lu, S.; Yan, K.; Yao, S. Energy absorption design study of subway vehicles based on a scaled equivalent model test. *Proc. Inst. Mech. Eng. Part F J. Rail Rapid Transit* **2019**, *233*, 3–15. [CrossRef]
13. Roh, J.S.; Ryou, H.S.; Park, W.H.; Jang, Y.J. CFD simulation and assessment of life safety in a subway train fire. *Tunn. Undergr. Space Technol.* **2009**, *24*, 447–453. [CrossRef]

14. Fernández, P.D.; Lindman, M.; Isaksson-Hellman, I.; Jeppsson, H.; Kovaceva, J. Description of same-direction car-to-bicycle crash scenarios using real-world data from Sweden, Germany, and a global crash database. *Accid. Anal. Prev.* **2022**, *168*, 106587. [CrossRef]
15. Peng, Y.; Chen, Y.; Yang, J.; Otte, D.; Willinger, R. A study of pedestrian and bicyclist exposure to head injury in passenger car collisions based on accident data and simulations. *Saf. Sci.* **2012**, *50*, 1749–1759. [CrossRef]
16. Arregui-Dalmases, C.; Kerrigan, J.R.; Sanchez-Molina, D.; Velazquez-Ameijide, J.; Crandall, J.R. A review of pelvic fractures in adult pedestrians: Experimental studies involving PMHS used to determine injury criteria for pedestrian dummies and component test procedures. *Traffic Inj. Prev.* **2015**, *16*, 62–69. [CrossRef] [PubMed]
17. Richardson, R.; Donlon, J.-P.; Jayathirtha, M.; Forman, J.L.; Shaw, G.; Gepner, B.; Kerrigan, J.R.; Östling, M.; Mroz, K.; Pipkorn, B. Kinematic and injury response of reclined PMHS in frontal impacts. *Stapp Car Crash J.* **2021**, *64*, 86–153.
18. Vavalle, N.A.; Jelen, B.C.; Moreno, D.P.; Stitzel, J.D.; Gayzik, F.S. An evaluation of objective rating methods for full-body finite element model comparison to PMHS tests. *Traffic Inj. Prev.* **2013**, *14*, S87–S94. [CrossRef] [PubMed]
19. Han, Y.; Yang, J.; Nishimoto, K.; Mizuno, K.; Matsui, Y.; Nakane, D.; Wanami, S.; Hitosugi, M. Finite element analysis of kinematic behaviour and injuries to pedestrians in vehicle collisions. *Int. J. Crashworth.* **2012**, *17*, 141–152. [CrossRef]
20. Shi, L.; Han, Y.; Huang, H.; Li, Q.; Wang, B.; Mizuno, K. Analysis of pedestrian-to-ground impact injury risk in vehicle-to-pedestrian collisions based on rotation angles. *J. Saf. Res.* **2018**, *64*, 37–47. [CrossRef]
21. Yu, C.; Wang, F.; Wang, B.; Li, G.; Li, F. A computational biomechanics human body model coupling finite element and multibody segments for assessment of head/brain injuries in car-to-pedestrian collisions. *Int. J. Environ. Res. Public Health* **2020**, *17*, 492. [CrossRef]
22. Zou, T.; Shang, S.; Simms, C. Potential benefits of controlled vehicle braking to reduce pedestrian ground contact injuries. *Accid. Anal. Prev.* **2019**, *129*, 94–107. [CrossRef]
23. Yin, S.; Li, J.; Xu, J. Exploring the mechanisms of vehicle front-end shape on pedestrian head injuries caused by ground impact. *Accid. Anal. Prev.* **2017**, *106*, 285–296. [CrossRef]
24. Tomsovsky, L.; Lopot, F.; Kubovy, P.; Jezdik, R.; Hajkova, B.; Rulc, V.; Jelen, K. Tram-pedestrian collisions: The severity of head injuries due to secondary impact with the surrounding infrastructure (ground). In Proceedings of the 2022 International Conference on Electrical, Computer, Communications and Mechatronics Engineering (ICECCME), Malé, Maldives, 16–18 November 2022; pp. 1–6.
25. Chevalier, M.-C.; Brizard, D.; Beillas, P. Study of the possible relationships between tramway front-end geometry and pedestrian injury risk. *Traffic Inj. Prev.* **2019**, *20*, 107–113. [CrossRef] [PubMed]
26. Hall, D.; Linogao, J.; Zentz, L.; Shaw, G.; Lamb, T.; Simms, C. Detailed Analysis of New York City Subway Pedestrian Incidents From 2019. *Transp. Res. Rec.* **2023**, *2677*, 642–650. [CrossRef]
27. Cocks, R.A. Study of 100 patients injured by London underground trains 1981-6. *Br. Med. J. (Clin. Res. Ed.)* **1987**, *295*, 1527–1529. [CrossRef] [PubMed]
28. O'Donnell, I.; Farmer, R. Suicidal acts on metro systems: An international perspective. *Acta Psychiatr. Scand.* **1992**, *86*, 60–63. [CrossRef] [PubMed]
29. O'Donnell, I.; Farmer, E. The epidemiology of suicide on the London Underground. *Soc. Sci. Med.* **1994**, *38*, 409–418. [CrossRef]
30. Coats, T.; Walter, D. Effect of station design on death in the London Underground: Observational study. *BMJ* **1999**, *319*, 957. [CrossRef]
31. Poirier, C.; Adelé, S.; Burkhardt, J.-M. Individual accidents at the interface between platform, train and tracks (PT 2 I) in the subway: A literature review. *Cogn. Technol. Work* **2021**, *23*, 203–224. [CrossRef]
32. Barker, E.; Kolves, K.; De Leo, D. Rail-suicide prevention: Systematic literature review of evidence-based activities. *Asia-Pac. Psychiatry* **2017**, *9*, e12246. [CrossRef]
33. New York City Transit. *System-Wide Platform Screen Door Feasibility Study*; The Metropolitan Transportation Authority: New York, NY, USA, 2020; p. 3920.
34. Kunitomi, S.; Takayama, S. Effect of pedestrian physique differences on head injury prediction in car-to-pedestrian accidents using deep learning. *Traffic Inj. Prev.* **2021**, *22*, S82–S86. [CrossRef]
35. Mizuno, K.; Horiki, M.; Zhao, Y.; Yoshida, A.; Wakabayashi, A.; Hosokawa, T.; Tanaka, Y.; Hosokawa, N. Analysis of fall kinematics and injury risks in ground impact in car-pedestrian collisions using impulse. *Accid. Anal. Prev.* **2022**, *176*, 106793. [CrossRef]
36. Gershon, R.R.; Pearson, J.M.; Nandi, V.; Vlahov, D.; Bucciarelli-Prann, A.; Tracy, M.; Tardiff, K.; Galea, S. Epidemiology of subway-related fatalities in New York City, 1990–2003. *J. Saf. Res.* **2008**, *39*, 583–588. [CrossRef] [PubMed]
37. Lin, P.T.; Gill, J.R. Subway Train-Related Fatalities in New York City: Accident versus Suicide. *J. Forensic Sci.* **2009**, *54*, 1414–1418. [CrossRef] [PubMed]
38. Zou, D.; Fan, Y.; Liu, N.; Zhang, J.; Liu, D.; Liu, Q.; Li, Z.; Wang, J.; Huang, J. Multiobjective optimization algorithm for accurate MADYMO reconstruction of vehicle-pedestrian accidents. *Front. Bioeng. Biotechnol.* **2022**, *10*, 1032621. [CrossRef] [PubMed]
39. Untaroiu, C.D.; Meissner, M.U.; Crandall, J.R.; Takahashi, Y.; Okamoto, M.; Ito, O. Crash reconstruction of pedestrian accidents using optimization techniques. *Int. J. Impact Eng.* **2009**, *36*, 210–219. [CrossRef]

40. Liu, J.; Rojas, J.; Li, Y.; Liang, Z.; Guan, Y.; Xi, N.; Zhu, H. A graph attention spatio-temporal convolutional network for 3D human pose estimation in video. In Proceedings of the 2021 IEEE International Conference on Robotics and Automation (ICRA), Xi'an, China, 30 May–5 June 2021; pp. 3374–3380.
41. Gildea, K.; Mercadal-Baudart, C.; Blythman, R.; Smolic, A.; Simms, C. KinePose: A temporally optimized inverse kinematics technique for 6DOF human pose estimation with biomechanical constraints. *arXiv* **2022**, arXiv:2207.12841.
42. Gildea, K.; Hall, D.; Cherry, C.R.; Simms, C. Forward dynamics computational modelling of a cyclist fall with the inclusion of protective response using deep learning-based human pose estimation. *J. Biomech.* **2024**, *163*, 111959. [CrossRef]
43. Li, G.; Yang, J.; Simms, C. Safer passenger car front shapes for pedestrians: A computational approach to reduce overall pedestrian injury risk in realistic impact scenarios. *Accid. Anal. Prev.* **2017**, *100*, 97–110. [CrossRef]
44. Versace, J. *A Review of the Severity Index*; SAE International: Warrendale, PA, USA, 1971.
45. Su, Y. *A Comparative Study of Pedestrian Fatalities and New Car Assessment Programs in the US and Japan*; Cornell University: Ithaca, NY, USA, 2019.
46. Suntay, B.; Stammen, J. *Assessment of Hood Designs for Pedestrian Head Protection: Active Hood Systems*; Department of Transportation. National Highway Traffic Safety Administration: Washington, DC, USA, 2020.
47. Hayes, W.C.; Erickson, M.S.; Power, E.D. Forensic injury biomechanics. *Annu. Rev. Biomed. Eng.* **2007**, *9*, 55–86. [CrossRef]
48. Li, G.; Yang, J.; Simms, C. The influence of gait stance on pedestrian lower limb injury risk. *Accid. Anal. Prev.* **2015**, *85*, 83–92. [CrossRef]